Search for Doubly Charged Higgs Boson Pair Production in the Decay to $\mu^+\mu^+\mu^-\mu^-$ in $p\bar{p}$ Collisions at $\sqrt{s} = 1.96$ TeV

V. M. Abazov,[32] B. Abbott,[69] M. Abolins,[60] B. S. Acharya,[26] D. L. Adams,[67] M. Adams,[47] T. Adams,[45] M. Agelou,[16] J.-L. Agram,[17] S. N. Ahmed,[31] S. H. Ahn,[28] G. D. Alexeev,[32] G. Alkhazov,[36] A. Alton,[59] G. Alverson,[58] G. A. Alves,[2] S. Anderson,[41] B. Andrieu,[15] Y. Arnoud,[12] A. Askew,[72] B. Åsman,[37] C. Autermann,[19] C. Avila,[7] L. Babukhadia,[66] T. C. Bacon,[39] A. Baden,[56] S. Baffioni,[13] B. Baldin,[46] P. W. Balm,[30] S. Banerjee,[26] E. Barberis,[58] P. Bargassa,[72] P. Baringer,[53] C. Barnes,[39] J. Barreto,[2] J. F. Bartlett,[46] U. Bassler,[15] D. Bauer,[50] A. Bean,[53] S. Beauceron,[15] F. Beaudette,[14] M. Begel,[65] S. B. Beri,[25] G. Bernardi,[15] I. Bertram,[38] M. Besançon,[16] A. Besson,[17] R. Beuselinck,[39] V. A. Bezzubov,[35] P. C. Bhat,[46] V. Bhatnagar,[25] M. Bhattacharjee,[66] M. Binder,[23] A. Bischoff,[44] K. M. Black,[57] I. Blackler,[39] G. Blazey,[48] F. Blekman,[30] D. Bloch,[17] U. Blumenschein,[21] A. Boehnlein,[46] T. A. Bolton,[54] P. Bonamy,[16] F. Borcherding,[46] G. Borissov,[38] K. Bos,[30] T. Bose,[64] C. Boswell,[44] A. Brandt,[71] G. Briskin,[70] R. Brock,[60] G. Brooijmans,[64] A. Bross,[46] D. Buchholz,[49] M. Buehler,[47] V. Buescher,[21] S. Burdin,[46] T. H. Burnett,[74] E. Busato,[15] J. M. Butler,[57] J. Bystricky,[16] F. Canelli,[65] W. Carvalho,[3] B. C. K. Casey,[70] D. Casey,[60] N. M. Cason,[51] H. Castilla-Valdez,[29] S. Chakrabarti,[26] D. Chakraborty,[48] K. M. Chan,[65] A. Chandra,[26] D. Chapin,[70] F. Charles,[17] E. Cheu,[41] L. Chevalier,[16] D. K. Cho,[65] S. Choi,[44] S. Chopra,[67] T. Christiansen,[23] L. Christofek,[53] D. Claes,[62] A. R. Clark,[42] C. Clément,[37] Y. Coadou,[5] D. J. Colling,[39] L. Coney,[51] B. Connolly,[45] W. E. Cooper,[46] D. Coppage,[53] M. Corcoran,[72] J. Coss,[18] A. Cothenet,[13] M.-C. Cousinou,[13] S. Crépé-Renaudin,[12] M. Cristetiu,[44] M. A. C. Cummings,[48] D. Cutts,[70] H. da Motta,[2] B. Davies,[38] G. Davies,[39] G. A. Davis,[65] K. De,[71] P. de Jong,[30] S. J. de Jong,[31] E. De La Cruz-Burelo,[29] C. De Oliveira Martins,[3] S. Dean,[40] K. Del Signore,[59] F. Déliot,[16] P. A. Delsart,[18] M. Demarteau,[46] R. Demina,[65] P. Demine,[16] D. Denisov,[46] S. P. Denisov,[35] S. Desai,[66] H. T. Diehl,[46] M. Diesburg,[46] M. Doidge,[38] H. Dong,[66] S. Doulas,[58] L. Duflot,[14] S. R. Dugad,[26] A. Duperrin,[13] J. Dyer,[60] A. Dyshkant,[48] M. Eads,[48] D. Edmunds,[60] T. Edwards,[40] J. Ellison,[44] J. Elmsheuser,[23] J. T. Eltzroth,[71] V. D. Elvira,[46] S. Eno,[56] P. Ermolov,[34] O. V. Eroshin,[35] J. Estrada,[46] D. Evans,[39] H. Evans,[64] A. Evdokimov,[33] V. N. Evdokimov,[35] J. Fast,[46] S. N. Fatakia,[57] D. Fein,[41] L. Feligioni,[57] T. Ferbel,[65] F. Fiedler,[23] F. Filthaut,[31] H. E. Fisk,[46] F. Fleuret,[15] M. Fortner,[48] H. Fox,[49] W. Freeman,[46] S. Fu,[64] S. Fuess,[46] C. F. Galea,[31] E. Gallas,[46] E. Galyaev,[51] M. Gao,[64] C. Garcia,[65] A. Garcia-Bellido,[74] J. Gardner,[53] V. Gavrilov,[33] D. Gelé,[17] R. Gelhaus,[44] K. Genser,[46] C. E. Gerber,[47] Y. Gershtein,[70] G. Geurkov,[70] G. Ginther,[65] K. Goldmann,[24] T. Golling,[20] B. Gómez,[7] K. Gounder,[46] A. Goussiou,[51] G. Graham,[56] P. D. Grannis,[66] S. Greder,[17] J. A. Green,[52] H. Greenlee,[46] Z. D. Greenwood,[55] E. M. Gregores,[4] S. Grinstein,[1] J.-F. Grivaz,[14] L. Groer,[64] S. Grünendahl,[46] M. W. Grünewald,[27] W. Gu,[6] S. N. Gurzhiev,[35] G. Gutierrez,[46] P. Gutierrez,[69] A. Haas,[74] N. J. Hadley,[56] H. Haggerty,[46] S. Hagopian,[45] I. Hall,[69] R. E. Hall,[43] C. Han,[59] L. Han,[40] K. Hanagaki,[46] P. Hanlet,[71] K. Harder,[54] J. M. Hauptman,[52] R. Hauser,[60] C. Hays,[64] J. Hays,[49] C. Hebert,[53] D. Hedin,[48] J. M. Heinmiller,[47] A. P. Heinson,[44] U. Heintz,[57] C. Hensel,[53] G. Hesketh,[58] M. D. Hildreth,[51] R. Hirosky,[73] J. D. Hobbs,[66] B. Hoeneisen,[11] M. Hohlfeld,[22] S. J. Hong,[28] R. Hooper,[51] S. Hou,[59] Y. Hu,[66] J. Huang,[50] Y. Huang,[59] I. Iashvili,[44] R. Illingworth,[46] A. S. Ito,[46] S. Jabeen,[53] M. Jaffré,[14] S. Jain,[69] V. Jain,[67] K. Jakobs,[21] A. Jenkins,[39] R. Jesik,[39] Y. Jiang,[59] K. Johns,[41] M. Johnson,[46] P. Johnson,[41] A. Jonckheere,[46] P. Jonsson,[39] H. Jöstlein,[46] A. Juste,[46] M. M. Kado,[42] D. Käfer,[19] W. Kahl,[54] S. Kahn,[67] E. Kajfasz,[13] A. M. Kalinin,[32] J. Kalk,[60] D. Karmanov,[34] J. Kasper,[57] D. Kau,[45] Z. Ke,[6] R. Kehoe,[60] S. Kermiche,[13] S. Kesisoglou,[70] A. Khanov,[65] A. Kharchilava,[51] Y. M. Kharzheev,[32] K. H. Kim,[28] B. Klima,[46] M. Klute,[20] J. M. Kohli,[25] M. Kopal,[69] V. Korablev,[35] J. Kotcher,[67] B. Kothari,[64] A. V. Kotwal,[64] A. Koubarovsky,[34] A. Kouchner,[16] O. Kouznetsov,[12] A. V. Kozelov,[35] J. Kozminski,[60] J. Krane,[52] M. R. Krishnaswamy,[26] S. Krzywdzinski,[46] M. Kubantsev,[54] S. Kuleshov,[33] Y. Kulik,[46] S. Kunori,[56] A. Kupco,[16] T. Kurča,[18] V. E. Kuznetsov,[44] S. Lager,[37] N. Lahrichi,[16] G. Landsberg,[70] J. Lazoflores,[45] A.-C. Le Bihan,[17] P. Lebrun,[18] S. W. Lee,[28] W. M. Lee,[45] A. Leflat,[34] C. Leggett,[42] F. Lehner,[46,*] C. Leonidopoulos,[64] P. Lewis,[39] J. Li,[71] Q. Z. Li,[46] X. Li,[6] J. G. R. Lima,[48] D. Lincoln,[46] S. L. Linn,[45] J. Linnemann,[60] R. Lipton,[46] L. Lobo,[39] A. Lobodenko,[36] M. Lokajicek,[10] A. Lounis,[17] J. Lu,[6] H. J. Lubatti,[74] A. Lucotte,[12] L. Lueking,[46] C. Luo,[50] M. Lynker,[51] A. L. Lyon,[46] A. K. A. Maciel,[48] R. J. Madaras,[42] A.-M. Magnan,[12] M. Maity,[57] P. K. Mal,[26] S. Malik,[55] V. L. Malyshev,[32] V. Manankov,[34] H. S. Mao,[6] Y. Maravin,[46] T. Marshall,[50] M. Martens,[46] M. I. Martin,[48] S. E. K. Mattingly,[70] A. A. Mayorov,[35] R. McCarthy,[66] R. McCroskey,[41] T. McMahon,[68] D. Meder,[22] H. L. Melanson,[46] A. Melnitchouk,[70] X. Meng,[6] M. Merkin,[34] K. W. Merritt,[46] A. Meyer,[19] C. Miao,[70] H. Miettinen,[72] D. Mihalcea,[48] C. S. Mishra,[46] J. Mitrevski,[64] N. Mokhov,[46] J. Molina,[3] N. K. Mondal,[26] H. E. Montgomery,[46] R. W. Moore,[5] M. Mostafa,[1] G. S. Muanza,[18] M. Mulders,[46] Y. D. Mutaf,[66] E. Nagy,[13] F. Nang,[41]

M. Narain,[57] V. S. Narasimham,[26] N. A. Naumann,[31] H. A. Neal,[59] J. P. Negret,[7] S. Nelson,[45] P. Neustroev,[36]
C. Noeding,[21] A. Nomerotski,[46] S. F. Novaes,[4] T. Nunnemann,[23] E. Nurse,[40] V. O'Dell,[46] D. C. O'Neil,[5] V. Oguri,[3]
N. Oliveira,[3] B. Olivier,[15] N. Oshima,[46] G. J. Otero y Garzón,[47] P. Padley,[72] K. Papageorgiou,[47] N. Parashar,[55] J. Park,[28]
S. K. Park,[28] J. Parsons,[64] R. Partridge,[70] N. Parua,[66] A. Patwa,[67] P. M. Perea,[44] E. Perez,[16] O. Peters,[30] P. Pétroff,[14]
M. Petteni,[39] L. Phaf,[30] R. Piegaia,[1] P. L. M. Podesta-Lerma,[29] V. M. Podstavkov,[46] B. G. Pope,[60] E. Popkov,[57]
W. L. Prado da Silva,[3] H. B. Prosper,[45] S. Protopopescu,[67] M. B. Przybycien,[49,†] J. Qian,[59] A. Quadt,[20] B. Quinn,[61]
K. J. Rani,[26] P. A. Rapidis,[46] P. N. Ratoff,[38] N.W. Reay,[54] J.-F. Renardy,[16] S. Reucroft,[58] J. Rha,[44] M. Ridel,[14]
M. Rijssenbeek,[66] I. Ripp-Baudot,[17] F. Rizatdinova,[54] C. Royon,[16] P. Rubinov,[46] R. Ruchti,[51] B. M. Sabirov,[32] G. Sajot,[12]
A. Sánchez-Hernández,[29] M. P. Sanders,[40] A. Santoro,[3] G. Savage,[46] L. Sawyer,[55] T. Scanlon,[39] R. D. Schamberger,[66]
H. Schellman,[49] P. Schieferdecker,[23] C. Schmitt,[24] A. Schukin,[35] A. Schwartzman,[63] R. Schwienhorst,[60] S. Sengupta,[45]
E. Shabalina,[47] V. Shary,[14] W. D. Shephard,[51] D. Shpakov,[58] R. A. Sidwell,[54] V. Simak,[9] V. Sirotenko,[46] D. Skow,[46]
P. Slattery,[65] R. P. Smith,[46] K. Smolek,[9] G. R. Snow,[62] J. Snow,[68] S. Snyder,[67] S. Söldner-Rembold,[40] X. Song,[48] Y. Song,[71]
L. Sonnenschein,[57] A. Sopczak,[38] V. Sorín,[1] M. Sosebee,[71] K. Soustruznik,[8] M. Souza,[2] N. R. Stanton,[54] J. Stark,[12]
J. Steele,[64] G. Steinbrück,[64] K. Stevenson,[50] V. Stolin,[33] A. Stone,[47] D. A. Stoyanova,[35] J. Strandberg,[37] M. A. Strang,[71]
M. Strauss,[69] R. Ströhmer,[23] M. Strovink,[42] L. Stutte,[46] A. Sznajder,[3] M. Talby,[13] P. Tamburello,[41] W. Taylor,[66]
P. Telford,[40] J. Temple,[41] S. Tentindo-Repond,[45] E. Thomas,[13] B. Thooris,[16] M. Tomoto,[46] T. Toole,[56] J. Torborg,[51]
S. Towers,[66] T. Trefzger,[22] S. Trincaz-Duvoid,[15] T. G. Trippe,[42] B. Tuchming,[16] A. S. Turcot,[67] P. M. Tuts,[64] L. Uvarov,[36]
S. Uvarov,[36] S. Uzunyan,[48] B. Vachon,[46] R. Van Kooten,[50] W. M. van Leeuwen,[30] N. Varelas,[47] E.W. Varnes,[41]
I. Vasilyev,[35] P. Verdier,[14] L. S. Vertogradov,[32] M. Verzocchi,[56] F. Villeneuve-Seguier,[39] J.-R. Vlimant,[15] E. Von Toerne,[54]
M. Vreeswijk,[30] T. Vu Anh,[14] H. D. Wahl,[45] R. Walker,[39] N. Wallace,[41] Z.-M. Wang,[66] J. Warchol,[51] M. Warsinsky,[20]
G. Watts,[74] M. Wayne,[51] M. Weber,[46] H. Weerts,[60] M. Wegner,[19] A. White,[71] V. White,[46] D. Whiteson,[42] D. Wicke,[24]
D. A. Wijngaarden,[31] G. W. Wilson,[53] S. J. Wimpenny,[44] J. Wittlin,[57] T. Wlodek,[71] M. Wobisch,[46] J. Womersley,[46]
D. R. Wood,[58] Z. Wu,[6] T. R. Wyatt,[40] Q. Xu,[59] N. Xuan,[51] R. Yamada,[46] T. Yasuda,[46] Y. A. Yatsunenko,[32] Y. Yen,[24] K. Yip,[67]
S.W. Youn,[28] J. Yu,[71] A. Yurkewicz,[60] A. Zabi,[14] A. Zatserklyaniy,[48] M. Zdrazil,[66] C. Zeitnitz,[22] B. Zhang,[6] D. Zhang,[46]
X. Zhang,[69] T. Zhao,[74] Z. Zhao,[59] H. Zheng,[51] B. Zhou,[59] Z. Zhou,[52] J. Zhu,[56] M. Zielinski,[65] D. Zieminska,[50]
A. Zieminski,[50] R. Zitoun,[66] V. Zutshi,[48] E. G. Zverev,[34] and A. Zylberstejn[16]

(D0 Collaboration)

[1]*Universidad de Buenos Aires, Buenos Aires, Argentina*
[2]*LAFEX, Centro Brasileiro de Pesquisas Físicas, Rio de Janeiro, Brazil*
[3]*Universidade do Estado do Rio de Janeiro, Rio de Janeiro, Brazil*
[4]*Instituto de Física Teórica, Universidade Estadual Paulista, São Paulo, Brazil*
[5]*University of Alberta, Edmonton, Canada, and Simon Fraser University, Burnaby, Canada*
[6]*Institute of High Energy Physics, Beijing, People's Republic of China*
[7]*Universidad de los Andes, Bogotá, Colombia*
[8]*Center for Particle Physics, Charles University, Prague, Czech Republic*
[9]*Czech Technical University, Prague, Czech Republic*
[10]*Institute of Physics, Academy of Sciences, Center for Particle Physics, Prague, Czech Republic*
[11]*Universidad San Francisco de Quito, Quito, Ecuador*
[12]*Laboratoire de Physique Subatomique et de Cosmologie, IN2P3-CNRS, Universite de Grenoble 1, Grenoble, France*
[13]*CPPM, IN2P3-CNRS, Université de la Méditerranée, Marseille, France*
[14]*Laboratoire de l'Accélérateur Linéaire, IN2P3-CNRS, Orsay, France*
[15]*LPNHE, Universités Paris VI and VII, IN2P3-CNRS, Paris, France*
[16]*DAPNIA/Service de Physique des Particules, CEA, Saclay, France*
[17]*IReS, IN2P3-CNRS, Université Louis Pasteur, Strasbourg, France and Université de Haute Alsace, Mulhouse, France*
[18]*Institut de Physique Nucléaire de Lyon, IN2P3-CNRS, Université Claude Bernard, Villeurbanne, France*
[19]*Physikalisches Institut A, RWTH Aachen, Aachen, Germany*
[20]*Physikalisches Institut, Universität Bonn, Bonn, Germany*
[21]*Physikalisches Institut, Universität Freiburg, Freiburg, Germany*
[22]*Institut für Physik, Universität Mainz, Mainz, Germany*
[23]*Ludwig-Maximilians-Universität München, München, Germany*
[24]*Fachbereich Physik, University of Wuppertal, Wuppertal, Germany*
[25]*Panjab University, Chandigarh, India*
[26]*Tata Institute of Fundamental Research, Mumbai, India*
[27]*University College Dublin, Dublin, Ireland*
[28]*Korea Detector Laboratory, Korea University, Seoul, Korea*

[29]CINVESTAV, Mexico City, Mexico

[30]FOM-Institute NIKHEF and University of Amsterdam/NIKHEF, Amsterdam, The Netherlands

[31]University of Nijmegen/NIKHEF, Nijmegen, The Netherlands

[32]Joint Institute for Nuclear Research, Dubna, Russia

[33]Institute for Theoretical and Experimental Physics, Moscow, Russia

[34]Moscow State University, Moscow, Russia

[35]Institute for High Energy Physics, Protvino, Russia

[36]Petersburg Nuclear Physics Institute, St. Petersburg, Russia

[37]Lund University, Lund, Sweden, Royal Institute of Technology and Stockholm University, Stockholm, Sweden,
and Uppsala University, Uppsala, Sweden

[38]Lancaster University, Lancaster, United Kingdom

[39]Imperial College, London, United Kingdom

[40]University of Manchester, Manchester, United Kingdom

[41]University of Arizona, Tucson, Arizona 85721, USA

[42]Lawrence Berkeley National Laboratory and University of California, Berkeley, California 94720, USA

[43]California State University, Fresno, California 93740, USA

[44]University of California, Riverside, California 92521, USA

[45]Florida State University, Tallahassee, Florida 32306, USA

[46]Fermi National Accelerator Laboratory, Batavia, Illinois 60510, USA

[47]University of Illinois at Chicago, Chicago, Illinois 60607, USA

[48]Northern Illinois University, DeKalb, Illinois 60115, USA

[49]Northwestern University, Eston, Illinois 60208, USA

[50]Indiana University, Bloomington, Indiana 47405, USA

[51]University of Notre Dame, Notre Dame, Indiana 46556, USA

[52]Iowa State University, Ames, Iowa 50011, USA

[53]University of Kansas, Lawrence, Kansas 66045, USA

[54]Kansas State University, Manhattan, Kansas 66506, USA

[55]Louisiana Tech University, Ruston, Louisiana 71272, USA

[56]University of Maryland, College Park, Maryland 20742, USA

[57]Boston University, Boston, Massachusetts 02215, USA

[58]Northeastern University, Boston, Massachusetts 02115, USA

[59]University of Michigan, Ann Arbor, Michigan 48109, USA

[60]Michigan State University, East Lansing, Michigan 48824, USA

[61]University of Mississippi, University, Mississippi 38677, USA

[62]University of Nebraska, Lincoln, Nebraska 68588, USA

[63]Princeton University, Princeton, New Jersey 08544, USA

[64]Columbia University, New York, New York 10027, USA

[65]University of Rochester, Rochester, New York 14627, USA

[66]State University of New York, Stony Brook, New York 11794, USA

[67]Brookhaven National Laboratory, Upton, New York 11973, USA

[68]Langston University, Langston, Oklahoma 73050, USA

[69]University of Oklahoma, Norman, Oklahoma 73019, USA

[70]Brown University, Providence, Rhode Island 02912, USA

[71]University of Texas, Arlington, Texas 76019, USA

[72]Rice University, Houston, Texas 77005, USA

[73]University of Virginia, Charlottesville, Virginia 22901, USA

[74]University of Washington, Seattle, Washington 98195, USA

A search for pair production of doubly charged Higgs bosons in the process $p\overline{p} \rightarrow H^{++}H^{--} \rightarrow \mu^{+}\mu^{+}\mu^{-}\mu^{-}$ is performed with the D0 run II detector at the Fermilab Tevatron. The analysis is based on a sample of inclusive dimuon data collected at an energy of $\sqrt{s} = 1.96$ TeV, corresponding to an integrated luminosity of 113 pb^{-1}. In the absence of a signal, 95% confidence level mass limits of $M(H_L^{\pm\pm}) > 118.4$ GeV/c^2 and $M(H_R^{\pm\pm}) > 98.2$ GeV/c^2 are set for left-handed and right-handed doubly charged Higgs bosons, respectively, assuming 100% branching into muon pairs.

Doubly-charged Higgs bosons appear in theories beyond the standard model, in particular, in left-right symmetric models [1], in Higgs triplet models [2], and in Little-Higgs models [3]. The models predict dominant decay modes to like-charge lepton pairs, $H^{\pm\pm} \rightarrow \ell^{\pm}\ell^{\pm}$. Pairs of doubly charged Higgs bosons can be produced through the Drell-Yan process $q\overline{q} \rightarrow \gamma^*/Z \rightarrow H^{++}H^{--}$. Next-to-leading order (NLO) corrections to this cross

section have recently been calculated [4]. The pair production cross sections for left-handed states in the mass range studied in this Letter are about a factor of 2 larger than for the right-handed states due to different coupling to the Z boson. Left-handed and right-handed states are distinguished through their decays into left-handed or right-handed leptons. The cross section also depends on the hypercharge Y of the $H^{\pm\pm}$ boson.

The $H^{\pm\pm}$ decay width into leptons is given by $\Gamma^{\ell\ell} = (8\pi)^{-1}|h_{\ell\ell}|^2 M_{H^{\pm\pm}}$, where $h_{\ell\ell}$ is the Yukawa coupling to leptons [2]. A limit on $h_{\mu\mu}^2/M_{H^{\pm\pm}}^2$, where $h_{\mu\mu}$ is the Yukawa coupling to muons, can be derived from the expected contribution to the anomalous magnetic moment of the muon, $(g-2)_\mu$ [5]. This yields upper limits on the Yukawa coupling $h_{\mu\mu}$ of the order of 0.1 for $M_{H^{\pm\pm}} = 100$ GeV/c^2. Requiring that $H^{\pm\pm}$ bosons decay within about 1 cm of their production restricts the sensitivity to $h_{\mu\mu}$ to approximately greater than 10^{-7}.

Experiments at the CERN e^+e^- collider LEP have searched for pair production of doubly charged Higgs bosons in e^+e^- interactions. Mass limits for decays into muons of $M(H_L^{\pm\pm}) > 100.5$ GeV/c^2 and $M(H_R^{\pm\pm}) > 100.1$ GeV/c^2 were obtained by the OPAL Collaboration [6], and a limit of $M(H_{L(R)}^{\pm\pm}) > 99.4$ GeV/c^2 by the L3 Collaboration [7]. Similar limits were set for decays into electrons [6,7] and τ leptons [6–8]. Our measurement represents the first $H^{\pm\pm}$ search at hadron colliders, and it extends significantly the range of sensitivity for left-handed doubly charged Higgs bosons decaying into muons. All limits in this Letter are given at 95% confidence level (C.L.).

The D0 run II detector comprises a central tracking system, a liquid-argon or uranium calorimeter, and an iron toroid muon spectrometer [9]. The central tracking system consists of a silicon microstrip tracker (SMT) and a central fiber tracker (CFT), both located within a 2 T superconducting solenoidal magnet. The SMT strips have a typical pitch of 50–80 μm and a design optimized for tracking and vertexing capability in the pseudorapidity range $|\eta| < 3$. The system has a six-barrel longitudinal structure, each with a set of four layers arranged axially around the beam pipe and interspersed with 16 radial disks. The CFT has eight thin coaxial barrels, each supporting two doublets of overlapping scintillating fibers of 0.835 mm diameter, one doublet being parallel to the collision axis, and the other alternating by $\pm 3°$ relative to the axis. The calorimeters consist of a central section covering (CC) $|\eta|$ up to ≈ 1 and two end calorimeters (EC) extending coverage to $|\eta| < 4.2$, all housed in separate cryostats [10]. Scintillators between the CC and EC cryostats provide sampling of showers at $1.1 < |\eta| < 1.4$. A muon system resides beyond the calorimetry and consists of a layer of tracking detectors and scintillation counters before 1.8 T iron toroids, followed by two more similar layers after the toroids. Tracking at $|\eta| < 1$ relies on 10 cm wide

drift tubes [10], while 1 cm minidrift tubes are used at $1 < |\eta| < 2$.

This analysis [11] is based on inclusive dimuon data recorded between August 2002 and June 2003. The events are triggered by requiring two muon candidates in the muon scintillation counters and at least one reconstructed muon using the muon wire chambers. The integrated luminosity is measured using two scintillator hodoscopes located on either side of the interaction region. For the dimuon triggers the integrated luminosity is 113 ± 7 pb^{-1}.

Event selection proceeds in four steps. The first step (selection S1) requires at least two muons. Each muon used in the analysis must have a transverse momentum $p_T > 15$ GeV/c, where p_T is measured with respect to the beam axis. The muon tracks are reconstructed using wire and scintillator hits in the different layers of the muon system. These must be combined successfully with a central track reconstructed in the SMT and CFT detectors to measure the muon momentum. A requirement on the timing of hits in different scintillator layers is used to minimize background from cosmic rays.

The second set of selections (S2) is based on isolation criteria based on calorimeter and tracking information and is designed primarily to reject background from muons originating from semileptonic B hadron decays. The direction of each muon track is projected through the calorimeter. For at least two muons, the sum of the transverse energies of the calorimeter cells in an annular ring $0.1 < R < 0.4$ around each muon direction is required to be $\sum_{\text{cells},i} E_T^i < 2.5$ GeV, where $R = \sqrt{(\Delta\phi)^2 + (\Delta\eta)^2}$ and ϕ is the azimuthal angle. In addition, the sum of the transverse momenta of all tracks other than that of the muon in a cone of $R = 0.5$ around the muon track is required to satisfy $\sum_{\text{tracks},i} p_T^i < 2.5$ GeV/c.

Selection (S3) applies to events with just two muons and requires a difference in azimuthal angle $\Delta\phi < 0.8\pi$. It is applied to reject $Z \to \mu^+\mu^-$ events and to reduce background from semileptonic B hadron decays. This selection also removes the remaining background from cosmic muons.

The final selection (S4) requires at least one pair of muons in the event to be of like-sign charge. These pairs are considered candidates for $H^{\pm\pm} \to \mu^\pm\mu^\pm$ decays.

The geometric and kinematic acceptance is taken from a GEANT-based [12] simulation of the detector. All other efficiencies are determined from $Z \to \mu^+\mu^-$ data. The single muon detection and reconstruction efficiencies and the efficiency of the isolation requirement are measured by using one muon to tag the event and the second muon to measure the efficiencies. The trigger efficiency is measured by analyzing events with calorimeter-based triggers which are independent of the muon system. To obtain the signal and background rates, corrections are applied to the simulation so that it reproduces the measured efficiencies. The total signal efficiency for our event selection is $(47.5 \pm 2.5)\%$ and does not depend on the
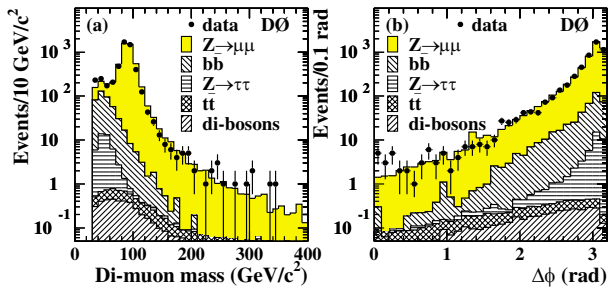
FIG. 1 (color online). Measured distribution of (a) dimuon mass and (b) $\Delta\phi$ compared to the sum of MC background processes after selection S1. Dimuon mass and $\Delta\phi$ are calculated for the two highest p_T muons, independent of their charge.

mass of the doubly charged Higgs boson in the mass range studied.

Distributions of the dimuon mass and of $\Delta\phi$ after selection S1 are shown in Fig. 1. The data are compared to the sum of Monte Carlo (MC) contributions from different background processes. In events with more than two muons, the dimuon mass and $\Delta\phi$ are calculated only for the two muons of highest p_T, independent of their charge. Both signal and background events are generated with PYTHIA 6.2 [13]. The next-to-next-to leading order cross section is used to normalize the $Z \to \mu^+\mu^-$ sample [14]. PYTHIA does not provide a good description of the jet multiplicity in Z + jets events. Since the $\Delta\phi$ distributions are expected to be sensitive to the number of jets, the simulated $Z \to \mu^+\mu^-$ events are reweighted to reproduce the distribution of jet multiplicities observed in data. There is agreement between data and the MC simulation, for both the normalization and shapes of the dimuon mass and $\Delta\phi$ distributions (Fig. 1). The number of events remaining after each selection and the efficien-

cies for a signal of a mass of $M(H_L^{\pm\pm}) = 100$ GeV/c^2 are given in Table I.

The background contribution from $t\bar{t}$ and diboson (WZ, ZZ, and WW) production is also estimated by the MC simulation. The NLO cross section is used for $t\bar{t}$ events [15]. Higher-order QCD corrections to diboson production are approximated by multiplying the LO cross section given in PYTHIA by a K factor of 1.34 [16]. Only the statistical uncertainties from the Monte Carlo generation are given for these background sources.

When the requirement of having at least one pair of like-charge muons is applied simultaneously with S1, most of the background from Z boson decays is removed, and only 101 like-sign events remain (Table II). Since no isolation requirement is imposed at this stage, the largest remaining background is from $b\bar{b}$ production. PYTHIA is used to estimate this background by generating inclusive jet events with a minimum transverse momentum of 30 GeV/c for the hard interaction. The inclusive b quark production cross section $\sigma^b(p_T^b > 30$ GeV/$c)$ was measured by D0 to be 54 ± 20 nb in the rapidity interval $|y^b| < 1$ at $\sqrt{s} = 1.8$ TeV [17]. This cross section is extrapolated via PYTHIA to the full y^b range and to $\sqrt{s} = 1.96$ TeV and is then used to normalize the $b\bar{b}$ MC sample.

Distributions in dimuon mass and $\Delta\phi$ for the like-sign events are compared to the PYTHIA $b\bar{b}$ simulation in Fig. 2. Since the data and the Monte Carlo simulation are in good agreement, the efficiency of the $\Delta\phi$ requirement is taken from the simulation. The data are used to determine the isolation efficiency. Out of 101 like-sign events, five remain after applying the isolation requirement (S2). Assuming that all like-sign events originate from $b\bar{b}$ processes, the isolation efficiency for $b\bar{b}$ events is found to be $(5 \pm 2)\%$, and the background from $b\bar{b}$ production in the final sample is expected to be 0.8 ± 0.3

TABLE I. The expected number of events for a signal with $M(H_L^{\pm\pm}) = 100$ GeV/c^2, background events from a Monte Carlo simulation for the available integrated data luminosity, and the number of observed events remaining after each selection cut. The simulation of Z decays includes the Drell-Yan contribution.

Selection	Two muons $p_T > 15$ GeV/c S1	Isolation S2	$\Delta\phi < 0.8\pi$ S3	Like sign S4
Signal	9.4	8.5	7.5	6.5
$Z \to \mu^+\mu^-$	4816	4055	359	0.3 ± 0.1
$b\bar{b}$	391	18	3.0	0.8 ± 0.4
$Z \to \tau^+\tau^-$	40	34	2.4	<0.1
$t\bar{t}$	3.0	2.1	1.5	0.11 ± 0.01
ZZ	0.1	0.1	0.1	0.05 ± 0.01
WZ	0.6	0.5	0.4	0.23 ± 0.01
WW	3.5	3.1	1.9	<0.01
Total background	5254 ± 47	4113 ± 43	368 ± 14	1.5 ± 0.4
Data	5168	4133	378	3

TABLE II. The expected number of background events from a Monte Carlo simulation for the available data luminosity, and the number of observed events remaining after each selection cut, with selection S4, requiring at least one like-charge muon pair, applied together with S1. The contribution from WW events is negligible.

Selection (Like-sign)	Two muons $p_T > 15$ GeV/c S4 & S1	Isolation S2	$\Delta\phi < 0.8\pi$ S3
$Z \to \mu^+\mu^-$	0.9 ± 0.3	0.6 ± 0.2	0.3 ± 0.1
$b\bar{b}$	95.1 ± 3.3	4.4 ± 1.9	0.8 ± 0.4
$Z \to \tau^+\tau^-$	<0.1	<0.1	<0.1
$t\bar{t}$	0.24 ± 0.01	0.11 ± 0.01	0.11 ± 0.01
ZZ	0.06 ± 0.01	0.05 ± 0.01	0.05 ± 0.01
WZ	0.29 ± 0.01	0.27 ± 0.01	0.23 ± 0.01
Total background	96.6 ± 3.3	5.4 ± 1.9	1.5 ± 0.4
Data	101	5	3

events. Adding a systematic uncertainty of 37% on the measured $b\bar{b}$ cross section [17] yields a total uncertainty on the $b\bar{b}$ background of 50%.

Another potential background is from $Z \to \mu^+\mu^-$ decays which are not rejected by the $\Delta\phi < 0.8\pi$ requirement and in which one of the muon charges is misidentified. For very high p_T tracks, the uncertainty on the measured curvature can cause such a flip of the track curvature. The probability for a charge misidentification increases with η, because there are fewer CFT layers in the region $|\eta| > 1.62$. The $Z \to \mu^+\mu^-$ simulation predicts 0.3 ± 0.1 events after the final selection. We have also estimated the probability for charge misidentification using data. The upper limit is given by the ratio of like-sign (5) to opposite sign (4133) events after the selection S2 (Tables I and II) and equals 0.12%. Since 378 events remain before the like-sign requirement, then assuming that the charge-misidentification probability is independent of the $\Delta\phi$ requirement, less than 0.5 ± 0.2 background events are expected due to charge misidentification. This is in good agreement with the simulation.

The production of W bosons decaying into $\mu\nu$, in association with jets, is another source of background, but mainly at low dimuon mass. By extrapolating to $p_T > 15$ GeV/c the steeply falling p_T spectrum of muons that fail the isolation requirements in dimuon events from a sample of $W \to \mu\nu$ + jets data, we estimate this contribution to be less than 0.1 events. The expected background rate, as determined from the data, is in agreement with the MC simulation.

Three candidates remain in the data after the final selection. The dimuon mass and $\Delta\phi$ distributions for these events are compared to the sum of MC backgrounds in Fig. 3. Two events have two negatively charged muons and one positively charged muon. Of the two, one has $\Delta\phi = 2.48$, and it has the highest like-sign dimuon mass (183 GeV/c^2) of the three candidates. The like-sign dimuon mass of the second event is 63 GeV/c^2 and the invariant mass of the two highest p_T muons of opposite charge in this event is 91 GeV/c^2. The third event has two positively charged muons with a mass of 62 GeV/c^2.

Since the remaining candidate events are consistent with a background observation, $H^{\pm\pm}$ mass limits are derived using the program MCLIMIT [18]. It provides the confidence level for the background to represent the data, CL_B, and the confidence level for the sum of signal and background hypothesis, CL_{S+B}, [19] taking into account the expected mass distribution for signal and background, and the mass resolution. The mass resolution varies between ≈ 7.6 GeV/c^2 for $M_{H^{\pm\pm}} = 80$ GeV/c^2 and ≈ 30 GeV/c^2 for $M_{H^{\pm\pm}} = 200$ GeV/c^2. The expected rate for the signal as a function of the Higgs mass is determined by the NLO cross section [4], the signal efficiencies, and the measured luminosity. The 95% C.L. limit for the signal is defined as $CL_S = CL_{S+B}/CL_B$, requiring $CL_S = 0.05$.

The following sources of systematic uncertainty affecting the normalization of the signal are taken into account: The systematic uncertainty on the luminosity is estimated
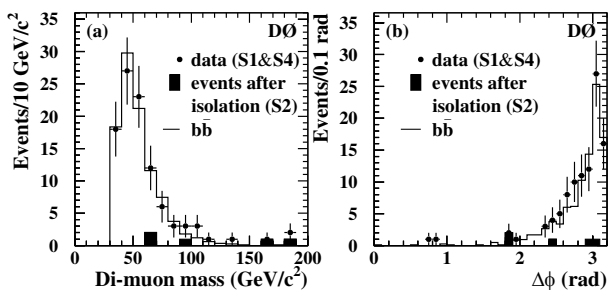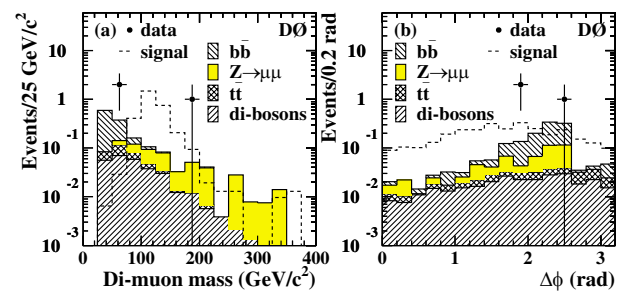

FIG. 2. (a) Dimuon mass and (b) $\Delta\phi$ for the two like-charge muons with the highest p_T. The 101 events remaining in the data after the selections S1 and S4 (points with error bars) are compared to the PYTHIA $b\bar{b}$ simulation (open histogram). The five data events remaining after the isolation selection are shown separately (full histogram).

FIG. 3 (color online). (a) Dimuon mass and (b) $\Delta\phi$ for the two like-charge muons of highest p_T. The data are compared to the sum of MC background processes after all selections. The open histogram shows the distributions for a left-handed, doubly charged Higgs boson with a mass of 120 GeV/c^2. Since the $\Delta\phi$ requirement is applied only to events with two muons, events with more than two muons can contribute for $\Delta\phi > 0.8\pi$.
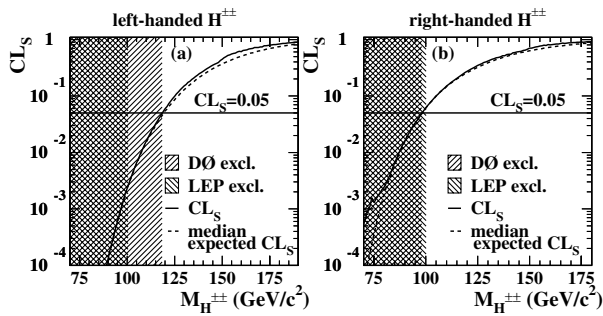
FIG. 4. Confidence level CL_S as a function of the mass $M_{H^{\pm\pm}}$ for (a) left-handed and (b) right-handed doubly charged Higgs bosons. Masses with $CL_S < 0.05$ are excluded by this analysis. The mass regions excluded by LEP are also shown. The impact of systematic uncertainties is included in the limits. The dashed curve shows the median expected CL_S for no signal.

to be 6.5%. The total uncertainty on the efficiency amounts to 5% and is dominated by the uncertainties on the efficiency to reconstruct an isolated muon and on the trigger efficiency. The uncertainty on the NLO $H^{\pm\pm}$ production cross section from choice of parton distribution functions and renormalization and factorization scales is about 10% [4]. The uncertainty on the background from the MC simulation is 27% (Table II). This includes the statistical uncertainty and the systematic uncertainty on the measured $b\bar{b}$ cross section [17].

The systematic uncertainties on signal and background are taken into account in the limit calculation through averaging over possible values of signal and background, as given by their probability distributions, which are assumed to be Gaussian [18]. This procedure weakens the limit on the mass by about 1 GeV/c^2. Other sources of systematic uncertainties, such as the interpolation procedure used for the cross sections and the description of the mass resolution, were examined and found to be negligible.

Figure 4 shows CL_S as a function of the mass of a doubly charged Higgs boson. The median expected CL_S indicates the sensitivity of the experiment for our luminosity, assuming that there is no signal. Taking into account systematic uncertainties, a lower mass limit of 118.4 GeV/c^2 is obtained for a left-handed and 98.2 GeV/c^2 for a right-handed doubly charged Higgs boson, assuming 100% branching into muon pairs, hypercharge $Y = |2|$, and Yukawa couplings $h_{\mu\mu} > 10^{-7}$. The limit on the cross section times branching ratio squared is 0.06 pb in the mass range between 80 and 135 GeV/c^2. This is the first search for doubly charged Higgs bosons at hadron colliders. It significantly extends the previous mass limit [6] for a left-handed doubly charged Higgs boson decaying into muons.

*Visitor from University of Zurich, Zurich, Switzerland.
†Visitor from Institute of Nuclear Physics, Krakow, Poland.

[1] J. C. Pati and A. Salam, Phys. Rev. D **10**, 275 (1974); R. N. Mohapatra and J. C. Pati, Phys. Rev. D **11**, 566 (1975); G. Senjanovic and R. N. Mohapatra, Phys. Rev. D **12**, 1502 (1975); T. G. Rizzo, Phys. Rev. D **25**, 1355 (1982); **27**, 657(A) (1983).

[2] See, for example, H. Georgi and M. Machacek, Nucl. Phys. **B262**, 463 (1985); J. F. Gunion, R. Vega, and J. Wudka, Phys. Rev. D **42**, 1673 (1990); J. F. Gunion, C. Loomis, and K. T. Pitts, hep-ph/9610237.

[3] N. Arkani-Hamed et al., J. High Energy Phys. 08 (2002) 021.

[4] M. Mühlleitner and M. Spira, Phys. Rev. D **68**, 117701 (2003); (private communication).

[5] A. J. Davies and X. G. He, Phys. Rev. D **43**, 225 (1991); K. Huitu et al., Nucl. Phys. **B487**, 27 (1997); F. Cuypers and S. Davidson, Eur. Phys. J. C **2**, 503 (1998); G. W. Bennett et al., Phys. Rev. Lett. **92**, 161802 (2004).

[6] OPAL Collaboration, G. Abbiendi et al., Phys. Lett. B **577**, 93 (2003); OPAL Collaboration, G. Abbiendi et al., Phys. Lett. B **526**, 221 (2002); OPAL Collaboration, P. D. Acton et al., Phys. Lett. B **295**, 347 (1992).

[7] L3 Collaboration, P. Achard et al., Phys. Lett. B **576**, 18 (2003).

[8] DELPHI Collaboration, J. Abdallah et al., Phys. Lett. B **552**, 127 (2003).

[9] D0 Collaboration, V. Abazov et al. (to be published); T. LeCompte and H. T. Diehl, Annu. Rev. Nucl. Part. Sci. **50**, 71 (2000).

[10] D0 Collaboration, S. Abachi et al., Nucl. Instrum. Methods Phys. Res., Sect. A **338**, 185 (1994).

[11] M. Zdražil, Ph.D. thesis, State University of New York, Stony Brook, 2004 (unpublished).

[12] R. Brun and F. Carminati, CERN Program Library Long Writeup No. W5013, 1993 (unpublished).

[13] T. Sjöstrand et al., Comput. Phys. Commun. **135**, 238 (2001).

[14] R. Hamberg, W. L. Neerven, and T. Matsuura, Nucl. Phys. **B359**, 343 (1991); **B644**, 403(E) (2002).

[15] N. Kidonakis, Phys. Rev. D **64**, 014009 (2001); N. Kidonakis, E. Laenen, S. Moch, and R. Vogt, Phys. Rev. D **64**, 114001 (2001).

[16] V. Barger, J. L Lopez, and W. Putikka, Int. J. Mod. Phys. A **3**, 2181 (1988).

[17] D0 Collaboration, S. Abachi *et al.*, Phys. Rev. Lett. **74**, 3548 (1995).

[18] T. Junk, Nucl. Instrum. Methods Phys. Res., Sect. A **434**, 435 (1999).

[19] ALEPH, DELPHI, L3, and OPAL Collaborations and the LEP Working Group for Higgs Boson Searches, R. Barate *et al.*, Phys. Lett. B **565**, 61 (2003).